Joint Special Interest Group meeting between euspen and ASPE
Advancing Precision in Additive Manufacturing
TU Berlin, Germany, October 2025
www.euspen.eu

Evaluating the Sensitivity of Optical Tomography and Melt Pool Monitoring Systems to LPBF Process Parameters

Kamel ETTAIEB[1], Noam MATTI[2], Didier BARDEL[3], Eleftherios ANAGNOSTOPOULOS[2]

[1]*Framatome, Centre Technique, France*
[2]*Framatome, Intercontrole, France*
[3]*Framatome, Fuel Design, France*

Kamel.ettaieb@framatome.com

Abstract
Laser Powder Bed Fusion (LPBF) is a technology that uses a laser to melt a powder bed layer by layer, enabling the production of complex components with high accuracy. This process offers new opportunities to reduce both the cost and the lead time for the manufacturing of critical parts in the nuclear industry. The high complexity of the produced components, particularly those with internal features, and the multi-physics phenomena involved during manufacturing, highlight the challenge of ensuring part quality for critical applications. In this context, in-situ monitoring systems have emerged as essential tools for process supervision, defect detection, and quality assurance.
This study investigates the impact of key LPBF process parameters on the signals captured by Optical Tomography (OT) and Melt Pool Monitoring (MPM) systems. A statistical analysis ANOVA (ANalysis Of Variance) is then used to perform a macroscopic evaluation, assessing how variations in laser power, scanning speed, and hatch distance influence the monitoring data. A Design of Experiments (DoE) was implemented to explore the sensitivity of in-situ monitoring signals as a function of variations in these parameters. The results reveal varying degrees of correlation between the selected parameters and the response of the monitoring signals, demonstrating the sensitivity and the potential of in-situ monitoring for tracking process stability. This work contributes to a better understanding of how process parameters influence monitoring outputs and supports future advancements in automated process control and anomaly detection in LPBF.

LPBF, process parameters, process control, in-situ monitoring, ANOVA

1. Introduction

LPBF process is increasingly used in a variety of industrial sectors due to its ability to manufacture components with highly complex geometries [1]. However, controlling such geometries remains challenging, and in some cases, such as internal channels in heat exchangers, it can be nearly impossible [2]. In this context, in-situ monitoring systems offer a promising solution to ensure process stability and part quality. These systems aim to provide insights into the build process helping to detect defects, particularly in cases where post-build inspection is limited or impossible. In addition, with the advent of new-generation LPBF machines, it is now possible to manufacture large-scale components, with build jobs lasting several weeks. While this capability significantly expands the range of applications for LPBF, it also increases the risks and costs associated with potential build failures. In this context, in-situ monitoring becomes even more critical, as it enables the early detection of defects during the manufacturing process. By identifying anomalies as they occur, it is possible to halt the build before completion, thereby avoiding the high costs associated with scrapping large, finished parts. This proactive approach contributes directly to reducing non-quality costs and improving overall process reliability.

Due to the inherent complexity of the LPBF process and the multitude of influencing parameters, establishing consistent correlations between defects and specific process conditions remains a significant challenge. To address this issue, many studies have applied artificial intelligence (AI) and machine learning (ML) to analyze in-situ monitoring signals and detect anomalies [3,4]. While these methods are effective at pattern recognition and defect classification, they come with key limitations. ML models often require large, high-quality labeled datasets and act as "black boxes," making it difficult to extract clear cause-effect relationships between process parameters and defects [5]. Moreover, the performance of in-situ monitoring systems and their ability to detect defects or parameter deviations during manufacturing strongly depend on system-specific characteristics, such as sensor resolution and acquisition frequency. Therefore, it is essential to understand each in-situ monitoring system and assess its sensitivity to process parameter variations to ensure reliable defect detection and effective control.

In this work, a statistical analysis using ANOVA (analysis of variance) is proposed to perform a macroscopic evaluation of the sensitivity of OT and MPM signals, from EOS in-situ monitoring systems, to variations in key process parameters: laser power, scanning speed, and hatch distance.

The rest of the paper is organized as following: Section 2 present the material and the proposed Experiment design. The Post-Processing and in-situ monitoring Data Analysis are presented in section 3. Section 4 is dedicated to the Statistical analysis of OT and MPM data. Finally, the paper ends with a conclusion and some perspectives

2. Material and methods

2.1. Machine and in-situ monitoring systems

The LPBF machine used in this study to manufacture the samples is the EOS M400-4. This machine employs four lasers to melt the powder layer across the entire surface of the baseplate. It is equipped by four in-situ monitoring systems integrated into the EOSTATE Suite: **EOSTATE System:** set of sensors installed in the machine to collect data as the temperature, oxygen level, humidity, etc.; **EOSTATE Powdered:** a CDD camera installed on the top of the build chamber. It takes a photo of the powder bed after recoating and laser exposure; **EOSTATE MeltPool:** on-axis photodiode records the melt pool radiation intensity around the small region of the melt pool; **EOSTATE Exposure OT:** an sCMOS-based camera with specially designed optics to gather high-resolution and high-focal depth images in the NIR wavelength range from the entire build platform during laser processing.

Only EOSTATE Exposure OT and MPM are used in this study.

2.2. Design of Experiments (DoE)

The principle of the proposed DoE is to manufacture geometries by deviating the primary process parameters from their standard values. The parameters studied are laser power (P), scanning speed (V), and hatch distance (H). Together with the layer thickness (E), these parameters determine the Volumetric Energy Density (VED) according to the following equation (1):

$$VED = \frac{P}{V \cdot H \cdot E} \qquad (1)$$

For each parameter, seven values are tested, as presented in Table 1. In total, 343 (7x7x7) VED configurations are evaluated. A constant value of layer thickness is maintained. The geometries are manufactured using 316L stainless steel.

Table 1. Synthesis of the values ranges of the tested parameters

Values ranges	Designations
Power (P): $0.7xP_N$, $0.8xP_N$, $0.9xP_N$, $\mathbf{P_N}$, $1.1xP_N$, $1.2xP_N$, $1.3xP_N$	P_N: standard P value
Scanning speed (V): $0.7xV_N$, $0.8xV_N$, $0.9xV_N$, $\mathbf{V_N}$, $1.1xV_N$, $1.2xV_N$, $1.3xV_N$	V_N: standard V value
Hatch distance (H): $0.7xH_N$, $0.8xH_N$, $0.9xH_N$, $\mathbf{H_N}$, $1.1xH_N$, $1.2xH_N$, $1.3xH_N$	H_N: standard H value

Six bars are manufactured. Each bar is composed of 58 sections, each with dimensions of 4 × 12 × 12 mm³. Each section is manufactured using a different VED value. The first section of each bar is produced using standard process parameters. Figure 2 presents the distribution of the VED for each section, as well as the position of each bar on the baseplate.

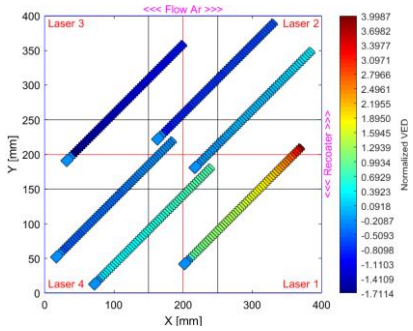

Figure 1. Distribution of the VED (normalized values) for each section

3. Post-Processing and in-situ monitoring Data Analysis

The EOSTATE software generates one OT mean image and one MPM mean image for each layer. The OT mean image of layer n corresponds to the average of all OT images captured during the melting of that layer. The MPM mean image of layer n is generated by averaging the signals recorded during the melting of the same layer. Figures 3 and 4 present the mean OT and MPM images, respectively, averaged over all layers.

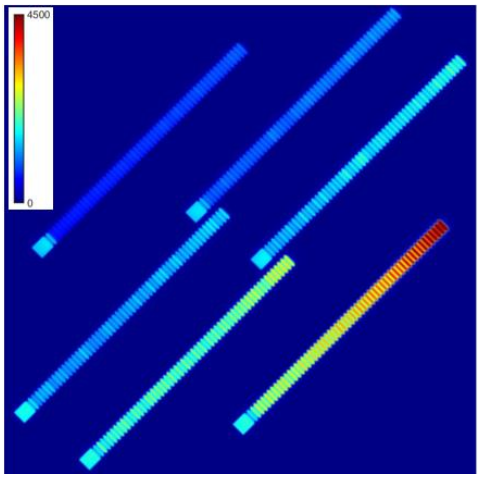

Figure 2. Average OT Mean per pixel

A clear correlation is observed between the evolution of the VED (figure 2) and the OT and MPM signals (figures 3 and 4). The increase in VED is detected by both the MPM and OT systems. Furthermore, the analysis of Figure 3 and Figure 4 reveals that the evolution of the OT signal as a function of VED is more clearly observable.

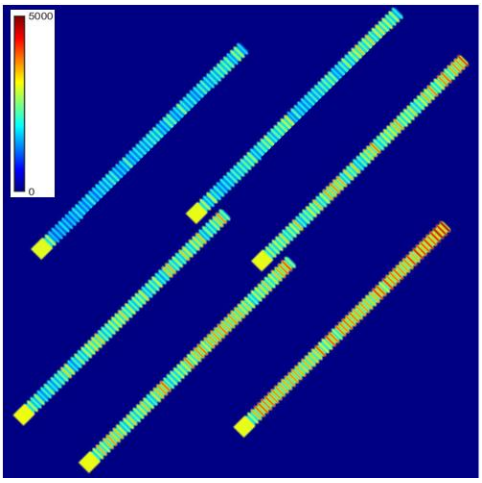

Figure 3. Average MPM Mean per pixel

In order to provide a more detailed analysis and study the impact of each tested process parameter, heat maps are generated. The objective is to study the evolution of MPM et OT signals in function of each tested parameter. The studied parameters are P, 1/V, and 1/H, which represent the logical decomposition of the terms in the VED formula. Figure 5 presents the heat maps of MPM and OT with normalized values. Each map illustrates the evolution of the MPM or OT signals as a function of two parameters. The value of each pixel (MPM or OT) corresponds to the average of the seven values obtained in the sections manufactured using the same value of the third parameter. For example, in the case of the P vs 1/V MPM heat map, the pixel at P = 1.51 and 1/V = 1.78 corresponds to the average of seven MPM mean values obtained with different 1/H

values, using sections manufactured with these fixed values of P and 1/V. The observations of the heat maps show that both OT and MPM signals vary with changes in the tested parameters.

MPM increases when the power increases and/or the scanning speed decreases. It is important to note that the MPM signal appears independent of the hatch distance (H) (figures 1/V vs 1/H and 1/H vs P (line 1)). In both cases, when the variable 1/H changes, the MPM signal remains nearly constant. In fact, given that the MPM system is co-axial with the laser beam, it captures signals from a local area at the center of the melt pool. It does not provide information on the thermal history after the laser has passed or between the beads.

OT signals vary with changes in each of the tested parameters: P, V, and H. As an off-axis system, OT captures the evolution of the thermal history across the entire surface of the baseplate. In addition, the OT signal appears more sensitive to variations in power (P) and scanning speed (V).

Heat maps illustrates the sensitivity of MPM and OT to the process parameters. The following section presents a statistical approach, ANOVA, to evaluate the influence of process parameters on the MPM and OT signals and to identify which parameters have a significant effect on the observed signal variations.

4. Statistical analysis of OT and MPM data

The statistical analysis aims to provide a macroscopic evaluation of the impact of the process parameter variations on MPM and OT signals. This involves studying the feasibility of developing linear regression models and determining which input parameters have a statistically significant impact on the output signals (OT and MPM).

4.1. Methodology

In this study, the input variables are the tested process parameters: P, V, and H. The natural variables, derived from the VED formula, are P, 1/V, and 1/H. Throughout the study, the selection of variables was progressively refined in order to enhance the accuracy and robustness of the regression models. The adopted approach is based on four main steps as follows:

1) **Data normalization:** This step aims to normalize all the studied data in order to ensure a consistent model.
2) **Linear regression:** this step aims to quantify the influence of the variables through a model of the form $Y = \sum A_i \cdot X_i$, where A_i are the linear coefficients, X_i the input variables, and Y the output variable.
3) **Analysis of Variance (ANOVA):** This step determines whether variations in the input variables significantly influence the output variable.
4) **Error and residual analysis:** Used to validate or reject the model.

4.2. Application on MPM mean data

The aim is to establish a model describing the MPM mean as a function of potentially influential parameters. The following formula presents the linear model that was tested. This model is defined as a function of the parameters that influence the VED (equation 2).

$$MPM\ mean = A_1 * P + A_2 * \frac{1}{V} + A_3 * \frac{1}{H} \qquad (2)$$

The linear regression and ANOVA methodology results is presented in Table 2.

Table 2. Linear regression and ANOVA results (MPM mean)

	Coef	Sdr err	t	p>|t|	[0.025	0.975]
P	0.8934	0.017	53.755	0.000	0.861	0.926
1/V	0.3961	0.016	24.068	0.000	0.364	0.429
1/H	0	-	-	-	-	-

Therefore, the resulting linear regression model for the MPM mean is as follows (Equation 3):

$$MPM\ Mean = 0.8934 * P + 0.3961 * \frac{1}{V} \qquad (3)$$

Figure 5 presents an overall summary of the results from the linear regression and ANOVA methodology.

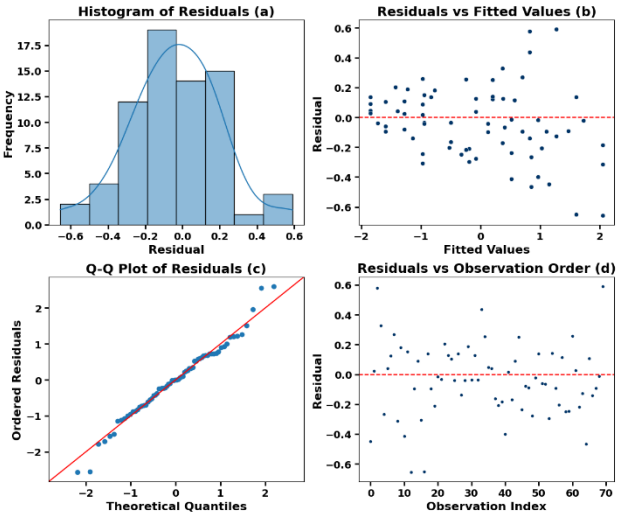

Figure 4. Residual analysis of the MPM Mean model

The results of this model are statistically significant at 95% confidence level. Moreover, the residuals (figure 5.c) show minimal deviation from the reference line in the Q-Q plot (Quantil-Quantil plot), and no pattern is observed in the residuals versus fitted values plot (figure 5.b). The analysis also shows that the average MPM signal value across all layers depends primarily on P and 1/V, which together explain 92.4% of the observed variation. This finding is consistent with the observations from the MPM mean heat map, which indicate that the MPM mean is not significantly affected by the hatch distance H.

4.3. Application on OT mean data

In a similar manner, a model is established for the OT mean. Table 3 presents the linear regression and the ANOVA results for OT Mean.

Table 3. Linear regression and ANOVA results (OT mean)

	Coef	Sdr err	t	p>|t|	[0.025	0.975]
P	0.4565	0.001	360.471	0.000	0.454	0.459
1/V	0.5905	0.001	465.895	0.000	0.588	0.593
1/H	0.5039	0.001	379.319	0.000	0.501	0.506

The linear regression model obtained for the OT mean is given by the following formula (Equation 4):

$$OT\ Mean = 0.45665 * P + 0.5905 * \frac{1}{V} + 0.5039 * \frac{1}{H} \qquad (4)$$

The residual analysis of the OT Mean model is presented in figure 6. Based on the residual analysis, this model was rejected due to the non-normality of the residuals, as evidenced by a strong deviation from the reference line in the Q-Q plot (figure 6.c) and a clear pattern in the residuals versus fitted values plot (figure 6.b). Moreover, the addition of a quadratic term and the

transformation of certain variables (such as logarithmic or exponential) failed to resolve the issue. However, as presented in Table 3, the high values of the Student's t-test (t) and p-values (p) below 5% confirm that the input parameters P, 1/V, and 1/H have a statistically significant influence.

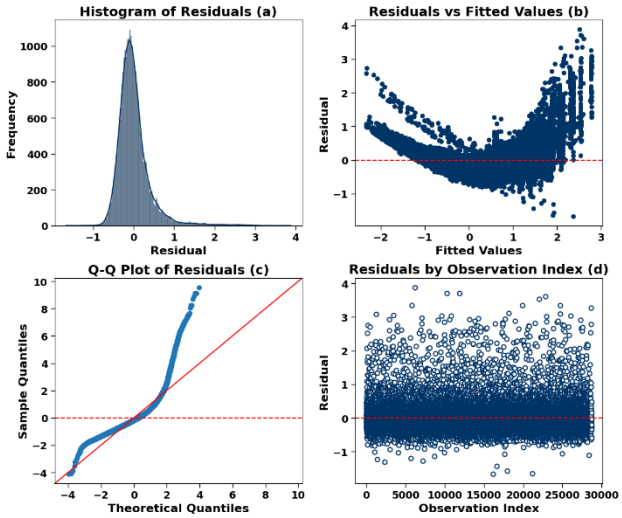

Figure 5. Residual analysis of the OT Mean model

Several combinations were tested, but none of the models provided a satisfactory fit for the OT mean. This might be explained by a non-linear relationship between the input variables (P, V and H) and the OT signal, or by the absence of other influential variables. In fact, the OT system is an off-axis system that captures the thermal history across the entire surface of the baseplate. The thermal evolution at each point is primarily influenced by the energy delivered by the laser when it passes over or near that point. Additionally, it is affected by heat conduction from other regions of the part. Furthermore, the thermal conditions may also be influenced by the atmospheric environment, which can be affected by other parameters such as the gas flow within the build chamber.

5. Conclusions and Future work

This study demonstrates the potential of in-situ monitoring systems, specifically the MPM and OT tools integrated into the EOS machine, to detect signal variations that reflect changes in process parameters.

The main findings of this study are: **(i)** The OT system, as an off-axis monitoring tool, captures signal that reflect variations in key process parameters such as laser power, scanning speed, and hatch distance. **(ii)** The MPM system, as an on-axis monitoring tool, detects deviations in laser power and scanning speed that influence the local melt pool region. However, it is not able to capture variations in hatch distance. **(iii)** The ANOVA analysis confirmed the previous findings, showing that laser power and scanning speed are the most influential parameters affecting the MPM signal, whereas the OT signal appears to be influenced by additional factors. While a satisfactory model was developed for the MPM signal, modeling the OT signal remains challenging due to residual non-normality and unexplained variability.

To validate these results of this study, CT-scan measurements on the manufactured samples have already been initiated. The objective is to establish a correlation between variations in process parameters, signals of the OT and MPM systems, and the defects detected in the manufactured samples.

References

[1] Blakey-Milner B, Gradl P, Snedden G, Brooks M, Pitot J, Lopez E, Leary M, Berto F, Plessis A,2021, Metal additive manufacturing in aerospace: A review, *J. Materials & Design*, vol. **209**, p.110008.

[2] Baier M, Sinico M, Witvrouw A, Dewulf W, Carmignato S, 2021, A novel tomographic characterisation approach for sag and dross defects in metal additively manufactured channels, *J. Additive Manufacturing*, vol. **39,** 101892.

[3] Mao Y et al. 2023, A deep learning framework for layer-wise porosity prediction in metal powder bed fusion using thermal signatures, *J. Journal of Intelligent Manufacturing*, vol. **34**, p. 315–329.

[4] Smoqi Z, Gaikwad A, Bevans B, Kobir MH, Craig J, Abul-Haj A, Peralta A, Rao P, 2022, Monitoring and prediction of porosity in laser powder bed fusion using physics-informed melt pool signatures and machine learning, *J. Materials & Design*, vol. **304,** 117550**.**

[5] Wahlquist S and Ali A, 2024, Roles of Modeling and Artificial Intelligence in LPBF Metal Print Defect Detection: Critical Review, *J. Applied Sciences,* Vol. **14**, 8534.

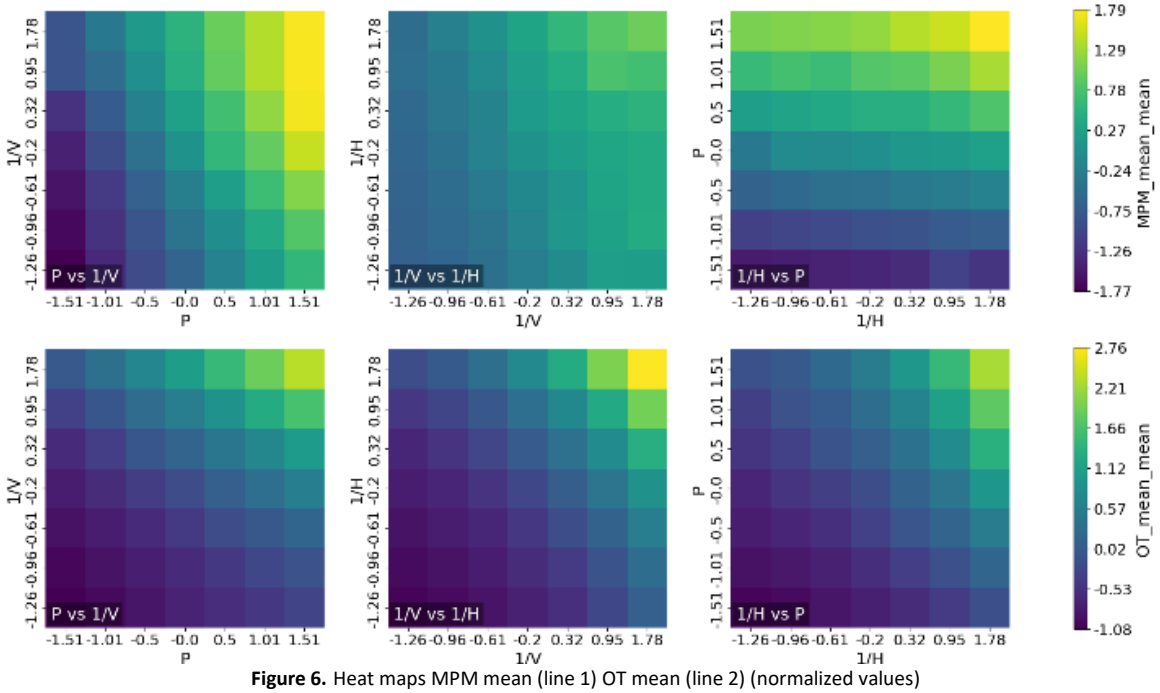

Figure 6. Heat maps MPM mean (line 1) OT mean (line 2) (normalized values)